A Kras^{G12D}-Driven Genetic Mouse Model of Pancreatic Cancer Requires Glypican-1 for Efficient Proliferation and Angiogenesis

Chery A. Whipple, Ph.D., **Alison L. Young, B.S., RLATG**, and **Murray Korc, M.D.**

Departments of Medicine and Pharmacology and Toxicology, Dartmouth Medical School, Hanover, NH 03755, USA; and the Norris Cotton Cancer Center at Dartmouth-Hitchcock Medical Center, Lebanon, NH 03756, USA

Abstract

Pancreatic ductal adenocarcinomas (PDACs) exhibit multiple molecular alterations and overexpress heparin binding growth factors (HBGFs) and glypican-1 (GPC1), a heparan sulfate proteoglycan that promotes efficient signaling by HBGFs. It is not known, however, whether GPC1 plays a role in genetic mouse models of PDAC. Therefore, we generated a GPC1 null mouse that combines pancreas-specific Cre-mediated activation of oncogenic Kras (Kras^{G12D}) with deletion of a conditional INK4A/Arf allele (Pdx1-Cre;LSL-Kras^{G12D};INK4A/Arf$^{lox/lox}$;GPC1$^{-/-}$ mice). By comparison with Pdx1-Cre;LSL-Kras^{G12D};INK4A/Arf$^{lox/lox}$ mice that were wild-type for GPC1, the Pdx1-Cre;LSL-Kras^{G12D};INK4A/Arf$^{lox/lox}$;GPC1$^{-/-}$ mice exhibited attenuated pancreatic tumor growth and invasiveness, decreased cancer cell proliferation and mitogen activated protein kinase (MAPK) activation. These mice also exhibited suppressed angiogenesis in conjunction with decreased expression of mRNAs encoding several pro-angiogenic factors and molecules, including vascular endothelial growth factor-A (VEGF-A), SRY-box containing gene (SOX17), chemokine C-X3-C motif ligand 1 (CX3CL1), and integrin β3 (ITGB3). Moreover, pancreatic cancer cells isolated from the tumors of GPC1$^{-/-}$ mice were not as invasive in response to fibroblast growth factor-2 (FGF-2) as cancer cells isolated from wild-type mice, and formed smaller tumors that exhibited an attenuated metastatic potential. Similarly, vascular endothelial growth factor-A (VEGF-A) and FGF-2 did not enhance the migration of hepatic endothelial cells and immortalized murine embryonic fibroblasts isolated from GPC1 null mice. These data demonstrate in an oncogenic Kras-driven genetic mouse model of PDAC that tumor growth, angiogenesis and invasion are enhanced by GPC1, and suggest that suppression of GPC1 may be an important component of therapeutic strategies in PDAC.

Keywords

Pancreatic cancer; glypican-1; proliferation; angiogenesis; tumor microenvironment

Correspondence to: Dr. M. Korc Department of Medicine One Medical Center Drive Dartmouth-Hitchcock Medical Center Lebanon, NH 03756, USA. Phone: (603) 653-9931 Fax: (603) 653-9952 murray.korc@dartmouth.edu.

Introduction

Pancreatic ductal adenocarcinoma (PDAC) is a highly metastatic malignancy that is the fourth leading cause of cancer death in the United States, with an overall five year survival rate of less than six percent (Siegel et al 2011). PDAC exhibits a wide range of genetic and epigenetic alterations including a high frequency (90-95%) of activating $Kras$ mutations, homozygous deletion (85%) and epigenetic silencing (15%) of the tumor suppressor genes p16^{INK4A}/p14^{ARF} (INK4A), as well as an over-abundance of heparin binding growth factors (HBGFs) (Korc 2003, Schneider and Schmid 2003). In spite of an improved understanding of these molecular alterations, there is a high incidence of treatment failure in PDAC, due, in part, to the resistance of pancreatic cancer cells to chemotherapy and radiotherapy (Kleeff et al 2007, Korc 2007, Schneider and Schmid 2003).

Many HBGFs, including fibroblast growth factor-2 (FGF-2), vascular endothelial growth factor (VEGF), platelet derived growth factor (PDGF), and hepatocyte growth factor (HGF) require the presence of the co-receptor glypican-1 (GPC1) for efficient signaling (Berman et al 1999, Chen and Lander 2001, Gengrinovitch et al 1999). GPC1 is a heparin sulfate proteoglycan (HSPG) that is attached to the plasma membrane of epithelial and stromal cells via a glycosylphophatidylinositol (GPI) anchor. GPC1, in conjunction with HBGFs, plays a critical role in cell growth, differentiation, adhesion, and, possibly, malignant transformation (Aikawa et al 2008, Blackhall et al 2001, Chen and Lander 2001, Kleeff et al 1998). GPC1 is overexpressed in PDAC and is required for efficient heparin binding growth factor signaling (Aikawa et al 2008, Kleeff et al 1998, Kleeff et al 1999).

Using athymic mice in a GPC1 null background and human pancreatic cancer cells in an orthotopic pancreatic cancer model, we have demonstrated that both host-derived and cancer cell-derived GPC1 contribute to enhanced tumor growth and metastasis in pancreatic cancer (Aikawa et al 2008, Kleeff et al 1998). It is not known, however, if GPC1 is important for both tumor initiation and progression in PDAC. Therefore, in the present study, we sought to investigate the impact of GPC1 on pancreatic tumor formation and growth in a transgenic mouse model that combines the latent LSL-Kras^{G12D} knock-in allele, the conditional INK4A$^{lox/lox}$ knockout allele, and either a GPC1 wild type (Pdx1-Cre;LSL-Kras^{G12D};INK4A/Arf$^{lox/lox}$;GPC1$^{+/+}$) or knockout (Pdx1-Cre;LSL-Kras^{G12D};INK4A/Arf$^{lox/lox}$; GPC1$^{-/-}$) allele.

We now report that the absence of GPC1 results in a significant decrease in tumor growth, invasiveness, angiogenesis, pancreatic cancer cell proliferation, and MAPK activation *in vivo*. *In vitro*, pancreatic cancer cells isolated from tumors arising in GPC1$^{-/-}$ transgenic mice exhibited attenuated invasion in response to FGF-2 by comparison to pancreatic cancer cells established from transgenic GPC1$^{+/+}$ mice. Additionally, primary hepatic endothelial cells and murine embryonic fibroblasts isolated from GPC1$^{-/-}$ mice were completely resistant to FGF-2-mediated migration. These findings indicate that endogenous GPC1 contributes to pancreatic cancer progression, even when driven by oncogenic Kras in conjunction with loss of INK4A, two highly prevalent alterations in PDAC.

Results

Creation of a novel transgenic mouse model

We generated a compound mouse model in which pancreas specific activation of endogenous Kras^{G12D} and the loss of pancreatic INK4A expression were combined with the complete absence of GPC1. To maintain a similar genetic background for both the GPC1 wild type (GPC1$^{+/+}$) and knockout (GPC1$^{-/-}$) transgenic mouse lines and to avoid lethality caused by homozygosity of either the mutant Kras or the Pdx1-Cre alleles (Johnson et al 1997), generation of the mouse model was carried out in a step-wise manner (Fig. S1). First, to create the GPC1$^{-/-}$ transgenic mouse, the mouse line carrying either the conditionally expressed LSL-Kras^{G12D} mutation or the INK4A$^{lox/lox}$ knockout allele was bred separately with GPC1$^{-/-}$ mice. In parallel, the mice harboring the INK4A$^{lox/lox}$ knockout allele and the Pdx1-Cre allele were bred to the GPC1$^{-/-}$ mouse line. Two rounds of breeding for each line produced mice that were either Pdx1-Cre;INK4A$^{Lox/Lox}$;GPC1$^{-/-}$ or LSL-Kras^{G12D};INK4A$^{Lox/Lox}$;GPC1$^{-/-}$. The offspring from these separate breeding strategies were crossed to produce Pdx1-Cre;LSL-Kras^{G12D};INK4A$^{Lox/Lox}$; GPC1$^{-/-}$ mice (Fig. S1). A similar breeding strategy was used to create the GPC1$^{+/+}$ transgenic mouse. Loss of INK4A and recombination of the mutant Kras allele were confirmed by genotyping all the mice.

Loss of GPC1 impacts tumor development and metastasis

To assess the impact of the loss of GPC1 on tumor development, we analyzed the pancreata of Pdx1-Cre;LSL-Kras^{G12D};INK4A$^{Lox/Lox}$;GPC1$^{-/-}$ and the corresponding GPC1$^{+/+}$ mice (Fig. 1). At 30 days of age, by gross analysis, only 1 of 10 GPC1$^{-/-}$ mice had developed a small pancreatic tumor versus 7 of the 10 GPC1$^{+/+}$ mice. In addition, the GPC1$^{-/-}$ pancreata were visibly smaller than the GPC1$^{+/+}$ pancreata (Fig. 1A), and the wet weight of the pancreata in GPC1$^{+/+}$ mice was significantly greater than in the GPC1$^{-/-}$ mice (Fig. 1B). At 65 days, 14 of 14 GPC1$^{+/+}$ transgenic mice harbored large and invasive pancreatic tumors that adhered to and invaded surrounding organs, whereas 4 of 20 GPC1$^{-/-}$ mice did not have any tumors, and the remaining 16 mice exhibited significantly smaller tumors that were not grossly invasive or adherent (Fig. 1 A-B). None of the mice exhibited grossly evident distant metastases.

Next, we carried out histological and immunohistochemical analysis of pancreata collected from GPC1$^{+/+}$ and GPC1$^{-/-}$ mice, using 10 pancreata per group from the 30 day old mice, and 14 pancreata per group from the 65 day old mice. Half of the compound transgenic mice developed pancreatic intraepithelial neoplasia (PanIN) lesions by 30 days of age and most of these were PanIN-1, -2 lesions (Sup. Table 1). By contrast, 3 of the 10 GPC1$^{+/+}$ mice exhibited PanIN-3 lesions, and one mouse had two separate invasive PDACs (Sup. Table 1), whereas only one of the 10 GPC1$^{-/-}$ mice displayed a PanIN-3 lesion, and none had a cancer. By day 65, 14 of 14 GPC1$^{+/+}$ and 13 of 14 GPC1$^{-/-}$ mice harbored invasive carcinomas. Although one GPC1$^{-/-}$ mouse did not have any PanIN or carcinoma, all of the transgenic mice displayed focal areas of acinar to ductal metaplasia (ADM lesions).

PanIN lesions in both GPC1$^{+/+}$ and GPC1$^{-/-}$ mice were histologically similar across all PanIN stages. Moreover, PanIN-1A lesions in both groups of mice displayed abundant

mucin production as evidenced by the presence of strong MUC1 immunoreactivity and Alcian blue staining (Fig. 1C). In addition, trichrome staining revealed that the stroma was similarly abundant in the tumors of both groups of mice (Fig. 1C). By contrast, Ki67 and CD34, which are markers for proliferation and angiogenesis, respectively (Le Mercier et al 2009, Vilar et al 2007), were markedly decreased in tumors from GPC1$^{-/-}$ by comparison with GPC$^{+/+}$ mice (Fig. 2). Immunofluorescent staining for Ki67 indicated that proliferation was significantly reduced in both the PanIN (CK19-positive) and stromal cells of tumors from 65 day old GPC1$^{-/-}$ transgenic mice (Fig. 3). Immunofluorescent staining for pMAPK was also decreased in the cancer cells within the tumors in GPC1$^{-/-}$ mice (Fig. 4), whereas caspase-3 staining was similar in both groups (data not shown). Q-PCR of tumor RNA isolated from 65 day old GPC$^{+/+}$ and GPC1$^{-/-}$ mice revealed that the loss of GPC1 did not significantly alter glypican-2, -3 -4, -5 or -6 levels (Fig. S2). By contrast, tumors arising from GPC1$^{-/-}$ pancreata expressed markedly reduced levels of VEGF-A mRNA by comparison with GPC1$^{+/+}$ tumors (Fig. S2).

To further delineate the role of GPC1 in pancreatic cancer progression, primary cancer cell lines were established from the tumors that arose in the GPC1$^{+/+}$ and GPC1$^{-/-}$ transgenic mice. Four murine pancreatic cancer cell lines were established, two from GPC1$^{+/+}$ (F1015 and F1048) and two from GPC1$^{-/-}$ (J444 and J1032) mice. Following subcutaneous injection in GPC1$^{+/+}$ nude mice, all four cell lines formed tumors. *In vitro*, F1015 and F1048 cells displayed significantly shorter doubling times (15 and 20 hours) than J444 and J1032 cells (30 and 24 hours), whereas J444 and J1032 cells exhibited decreased invasiveness in response to FGF-2 by comparison with either F1015 or F1048 cells (Fig. 5).

Given that loss of GPC1 reduced doubling times and invasion *in vitro*, we next sought to determine whether GPC1 also modulated the metastatic potential of pancreatic cancer cells. Accordingly, small (2 mm^3) fragments were prepared from 65 day old GPC1$^{+/+}$ and GPC1$^{-/-}$ mice, and implanted, respectively, into the pancreata of athymic GPC1$^{+/+}$ and GPC1$^{-/-}$ mice. Tumor growth arising from transplanted fragments reflects the influence of both transplanted cancer cells and associated stroma, and yields metastatic lesions. Dramatically, two weeks following fragment implantation, only 2 of 14 GPC1$^{-/-}$ mice developed metastases, which were confined to the mesentery, whereas 9 of 15 GPC1$^{+/+}$ mice developed numerous (over 100 per mouse) mesenteric metastases and 3 of these mice also exhibited multiple renal metastases (Table 1).

The implanted tumor fragments contained cancer-associated fibroblasts and endothelial cells, which may help to promote a pro-metastatic profile. Therefore, we next sought to assess the impact of GPC1 loss on fibroblast and endothelial cell function. In a first set of experiments, MEFs were isolated from GPC1$^{+/+}$ or GPC1$^{-/-}$ mice at embryonic day 14.5, and immortalized by stable infection with a retroviral vector containing a dominant negative p53 mutation. The immortalized MEFs were readily maintained in culture. In contrast to wild-type MEFs, GPC1$^{-/-}$ MEFs failed to respond to FGF-2 in a migration assay, even when the ligand concentration was increased 5-fold (Fig. 6). In a second set of experiments, the effects of VEGF-A on primary endothelial cells isolated from GPC1$^{+/+}$ or GPC1$^{-/-}$ mice were studied in a transwell migration assay. VEGF-A significantly increased the migration of GPC1$^{+/+}$-derived endothelial cells, but did not alter the migration of GPC1$^{-/-}$-derived

endothelial cells (Fig. 6). Thus, both fibroblasts and endothelial cells derived from GPC1$^{-/-}$ mice were less responsive to HBGFs.

In view of the lower level of VEGF-A in GPC1$^{-/-}$-derived tumors and the decreased migration of endothelial cells from these mice, we next sought to determine whether the loss of GPC1 altered the expression of angiogenic genes. Microarray analysis of RNA extracted from transgenic tumors isolated from 65 day old mice indicated that six other pro-angiogenic genes were also expressed at low levels in the absence of GPC1. Thus, SRY-box containing gene (SOX17), chemokine C-X3-C motif ligand 1 (CX3CL1), ephrin-A1 (EFNA1), guanine nucleotide binding protein alpha 13 (GNA13), integrin beta 3 (ITGB3), protein tyrosine kinase 2 beta (PTK2B), and VEGF-A mRNA levels were expressed at a significantly lower level in the GPC1$^{-/-}$ tumors (Table 2 and Fig. S3). By contrast, the expression of angiostatic genes, such as tissue inhibitor of metalloproteinases (TIMP)-1 and -2, nm23, angiopoietin-2, thrombospondin-2, or prolactin, was similar in both groups of pancreata (data not shown).

Discussion

Several lines of evidence suggest that GPC1 may have an important role in PDAC. First, studies with human pancreatic cancer cell lines injected subcutaneously in athymic mice have demonstrated that GPC1 expression is required for efficient pancreatic tumor growth and angiogenesis (Kleeff et al 1998, Kleeff et al 1999). Second, GPC1 is overexpressed in resected PDAC samples, and both the cancer cells and the cancer-associated fibroblasts express GPC1 at the mRNA and protein level (Kleeff et al 1998), indicating that both cell types synthesize GPC1. Third, GPC1 is abundant in the stroma adjacent to the cancer cells in PDAC, and *in vitro* studies with human pancreatic cancer cell lines have shown that GPC1 is readily released by these cells (Matsuda et al 2001), pointing to a possible role for GPC1 within the tumor microenvironment. Fourth, studies with athymic GPC1$^{-/-}$ mice have demonstrated that host-derived GPC1, produced by stromal and endothelial cells, contributes to pancreatic tumor growth, metastasis, and angiogenesis (Aikawa et al 2008). Fifth, gene expression profiling in pancreatic intraductal papillary-mucinous tumors (IPMTs) revealed that GPC1 is upregulated in these lesions, but nearly exclusively in invasive IPMTs, suggesting a potential role in tumor invasion (Terris et al 2002).

The LSL-Kras^{G12D} mouse, which we combined with the loss of both GPC1 and INK4A, carries an oncogenic Kras (Kras^{G12D}) allele that has been knocked-in within its own locus but which is transcriptionally silenced by the insertion of a LoxP-Stop-LoxP element (LSL) located upstream of the transcriptional start site (Aguirre et al 2003, Hingorani et al 2003). Oncogenic Kras expression remains under the control of its own endogenous promoter, and the transcript is produced only in early pancreatic progenitor cells after excision of the LSL sequence via the Pdx-1 driven Cre recombinase. The Pdx1-Cre;LSL-Kras^{G12D} mice develop low grade PanIN and exhibit areas of acinar to ductal metaplasia by 2 months of age (Aguirre et al 2003). When the mice are 8 to 12 months old, they develop PDAC at low penetrance (Aguirre et al 2003, Habbe et al 2008). PanIN progression to pancreatic cancer is an important feature of PDAC initiation in both human and mouse models and is dramatically accelerated in Pdx1-Cre;LSL-Kras^{G12D};INK4A$^{lox/lox}$ mice. In addition to

harboring oncogenic $Kras^{G12D}$, the pancreata of these mice have sustained a homozygous deletion of the INK4A locus, resulting in large, highly invasive tumors by 7-11 weeks of age (Aguirre et al 2003, Jackson et al 2001).

In the present study, both 30 and 65 day old Pdx1-Cre;LSL-$Kras^{G12D}$;INK4A$^{Lox/Lox}$;GPC1$^{-/-}$ mice displayed significantly smaller tumors than the corresponding GPC1$^{+/+}$ mice. PanIN appeared at the same time in both groups of mice and were morphologically similar, exhibiting similar patterns of MUC1 and alcian blue staining. Nonetheless, proliferation markers were increased in the PanIN lesions in GPC1$^{+/+}$ mice by comparison with GPC1$^{-/-}$ mice. Moreover, PanIN progression from PanIN-1 to PanIN-3 lesions and to PDAC occurred more rapidly in the GPC1$^{+/+}$ mice. Thus, GPC1 is not required for PanIN initiation but acts to promote progression toward malignancy, most likely by facilitating epithelial cell proliferation within these lesions.

The cancer cells and the cancer associated fibroblasts in GPC1$^{+/+}$ mouse tumors also exhibited increased proliferation and elevated phospho-MAPK levels, indicating that GPC1 enhances mitogenic signaling in both cell types. By contrast, Mason's-Trichrome and caspase-3 staining were similar in tumors from GPC1$^{+/+}$ and GPC1$^{-/-}$ mice, suggesting that GPC1 promoted larger tumors by facilitating enhanced proliferation of the cancer cells rather than by promoting increased collagen deposition or attenuating apoptosis. In support of this conclusion, primary cancer cells derived from the GPC1$^{+/+}$ mice exhibited enhanced proliferation *in vitro*. Inasmuch as GPC1 is devoid of intrinsic signaling activity, these observations suggest that GPC1 may act by a cell-autonomous manner to facilitate autocrine growth stimulation elicited by cancer cell-derived HBGFs that act via their cognate high-affinity receptors.

Recent studies underscore the importance of the cancer-associated stroma in facilitating tumor spread, invasion, and metastasis, enhancing chemoresistance and promoting apoptosis resistance (Hwang et al 2008, Vonlaufen et al 2008). PDAC is characterized by an abundant desmoplastic reaction that is rich in collagen I, pancreatic stellate cells (PSCs), fibroblasts, and inflammatory cells, which collectively promote cancer cell growth and invasiveness and contribute to chemoresistance (Kleeff et al 2007). While orthotopic models of PDAC have generally not been associated with desmoplasia, many genetic mouse models of PDAC, including the Pdx1-Cre;LSL-$Kras^{G12D}$;INK4A/Arf$^{lox/lox}$ mice used in the current study, exhibit desmoplasia (Aguirre et al 2003, Tuveson and Hingorani 2005). By contrast, orthotopic models exhibit aberrant angiogenesis (Rowland-Goldsmith et al 2002), whereas genetic mouse models of PDAC are ostensibly not angiogenesis-dependent and consequently are more resistant to chemotherapy (Olive et al 2009). It is noteworthy, therefore, that there was abundant angiogenesis in the tumors arising in Pdx1-Cre;LSL-$Kras^{G12D}$;INK4A/Arf$^{lox/lox}$;GPC1$^{+/+}$ mice, and that tumors in GPC1$^{-/-}$ pancreata displayed markedly reduced angiogenesis. Thus, tumor angiogenesis is important in at least some genetic mouse model of PDAC, is driven by GPC1-dependent mechanisms, and can contribute to enhanced pancreatic cancer growth and metastasis. This pre-clinical model could therefore be useful for assessing the effectiveness of specific anti-angiogenic therapeutic modalities in PDAC, and for investigating the mechanisms that contribute to the failure of anti-angiogenic therapy in clinical trials (Preis and Korc 2010).

At least six mechanisms may underlie the ability of GPC1 to promote tumor angiogenesis in Pdx1-Cre;LSL-Kras^{G12D};INK4A/Arf$^{lox/lox}$ mice. First, the GPC1$^{-/-}$ tumors exhibited decreased expression of VEGF-A, a potent pro-angiogenic factor. Second, our array studies revealed that there was concomitant down-regulation of six additional genes implicated in promoting angiogenesis, such as integrin β3 and ephrin-A1. By contrast, the expression of angiostatic genes was similar in both groups of pancreata. Inasmuch as VEGF-A is known to up-regulate the expression of ephrin-A1 (Cheng et al 2002), it is possible that loss of GPC1, by leading to decreased VEGF-A expression and function, results in the down-regulation of downstream genes such as ephrin-A1, further impeding angiogenesis. Third, there was a marked decrease in Sox17 mRNA levels in tumors from GPC1$^{-/-}$ mice. Sox17 is a transcriptional regulator that is expressed in fetal and neonatal hematopoietic stem cells (HSCs), but not in adult HSCs (Kim et al 2007). Inasmuch as HSCs have been implicated in PDAC angiogenesis (Li et al 2011) it is possible that GPC1 is also important for PDAC's ability to recruit HSCs to promote tumor angiogenesis. Fourth, by contrast to endothelial cells isolated from GPC1$^{+/+}$ mice, endothelial cells from GPC1$^{-/-}$ mice did not migrate in response to VEGF-A, underscoring the GPC1-dependence for efficient VEGF-A signaling. Fifth, GPC1 may also act to promote growth factor sequestration within the tumor microenvironment, enhancing their stability and ability to act as morphogens (Lander et al 2002, Vlodavsky et al 1990). Thus, the absence of GPC1 within the tumors of GPC1$^{-/-}$ mice may decrease the pool of heparan sulfate side chains, thereby decreasing the amount of stored HBGFs, such as VEGF-A (41, 42), that can be released by the actions of the endoglycosidase heparanase, which is up-regulated in PDAC (Zetser et al 2006). Sixth, the absence of GPC1 may also interfere with the shedding of active MMP7 (Ding et al 2005), which acts to release all stored growth factors, irrespective of their heparin-binding ability. Together, these observations suggest that GPC1 may be an important component of a pro-angiogenic switch in PDAC.

Using athymic mice, both host-derived and cancer cell-derived GPC1 has been shown to contribute to enhanced pancreatic cancer growth (Aikawa et al 2008, Kleeff et al 1998). In the present study, pancreatic cancer cell lines established from GPC1$^{-/-}$ mice demonstrated a marked decrease in invasiveness *in vitro*, as well as attenuated growth and metastatic potential following intra-pancreatic implantation in GPC1 deficient nude mice. Thus, in the absence of GPC1, pancreatic cancer cells derived from Kras-driven genetic mouse model of PDAC exhibit attenuated tumor progression, angiogenesis, invasiveness, and metastasis, suggesting that targeting GPC1 either alone or in combination with mitogenesis and/or angiogenesis inhibitors may help to overcome the resistance to Kras-targeted therapeutic strategies.

Materials and Methods

Mouse colony generation

LSL-Kras^{G12D};INK4A/Arf$^{Lox/Lox}$;SMAD4$^{lox/lox}$ and Pdx1-Cre mice strains were kindly provided by Nabeel Bardeesy at Harvard University (Bardeesy et al 2006) and Guo Gu at Vanderbilt University (Gu et al 2003), respectively. The SMAD4$^{lox/lox}$ mutation was bred out of this line prior to introducing the Pdx1-Cre and GPC1 mutations (Fig. S1). The

GPC1$^{-/-}$ mice were produced by targeted mutagenesis as described previously (Aikawa et al 2008, Jen et al 2009). All mice were genotyped twice by PCR to verify the presence of each transgene.

Histology and immunohistochemistry of paraffin embedded tissues

Pancreatic tissues were fixed for 6-12 hours in 10% formalin, embedded in paraffin, sectioned (5 μm thick), mounted on poly-L-lysine-coated glass slides, and incubated at 79°C for 30 minutes. After deparaffinization, antigen retrieval was performed by using the 2100-Retriever (PickCell Laboratories, Amsterdam, The Netherlands) and antigen unmasking solution (pH 6.0). Sections were washed in PBS, incubated for 10 min with 3% H_2O_2 to block endogenous peroxidase activity, washed in PBS with 0.025% Triton-X, incubated for one hour in blocking buffer (1% BSA and 5% normal goat or horse serum), and overnight at 4°C with the appropriate monoclonal antibody (Aguirre et al 2003, Aikawa et al 2008). Bound antibody was detected with the suitable biotinylated secondary antibody (1:500) and VECTASTAIN ABC Reagent (Vector Laboratories, Burlingame, CA) complex, using diaminobenzidine tetrahydrochloride (DAB) as the substrate (Rowland-Goldsmith et al 2002).

The following primary antibodies were used: anti-Ki67 (Novocastra, Bannockburn, IL), 1:100; anti-cleaved caspase-3 (Cell Signaling Technology, Beverly MA), 1:200; anti-MUC1 (Abcam Inc, Cambridge, MA), 1:1000; TromaIII (anti-CK19 antibody developed by Rolf Kemler and obtained from the Developmental Studies HybridomaBank, Iowa City, IA), 1:10; anti-Cd34 (Abcam Inc, Cambridge, MA), 1:25; and anti-phospho-MAPK (Cell Signaling Technology, Danvers, MA), 1:500. Negative controls without primary antibodies did not exhibit immunoreactivity. Pictures were captured on an Olympus BX60 microscope with a QImaging EXI Blue camera utilizing 10X and 20X objectives. Quantitative morphometry was performed with Image-Pro® Plus 7 (Media Cybernetics, Silver Springs, MD), as previously reported (11).

Isolation of primary cell lines

To isolate and establish primary cancer cell lines, pancreatic tumors were rapidly harvested from Pdx1-Cre;LSL-Kras^{G12D};INK4A$^{Lox/Lox}$;GPC1$^{+/+}$ or GPC1$^{-/-}$ transgenic mice that were 60 to 65 days old (Seeley et al 2009). The tumors were minced with sterile scissors, digested with collagenase IV (2.5 mg/ml) for 1 h at 37°C, and resuspended in cancer cell growth media (RPMI 1640 with 20% FBS, 100 units/ml penicillin/streptomycin). The cell mixture was laid over an equal volume of histopaque, and spun for 15 minutes at 2000 rpm. The pellet was isolated, resuspended in cancer cell growth medium, and seeded on tissue culture plates.

Primary mouse embryo fibroblasts (MEFs) were isolated from 13.5-day-old embryos (Xu 2005) and placed in growth medium consisting of DMEM containing 8% FBS, 100 units/ml penicillin/streptomycin, and 25 ng/ml amphotericin B, plated on tissue culture plates and incubated at 37°C with 5% CO_2. At cell passage two, MEFs isolated from GPC1$^{+/+}$ or GPC1$^{-/-}$ mice were immortalized with a p53 dominant negative retroviral vector (a gift from

Robert Weinberg, Whitehead Institute, Cambridge, MA), utilizing standard retroviral infection protocols (Cepko 1996).

Primary endothelial cells were isolated from adult livers as described previously (13), using Dynalbeads (Invitrogen) labeled with anti-CD31 antibodies (Aikawa et al 2008). Endothelial cells were similarly isolated from tumors arising in Pdx1-Cre;LSL-Kras^{G12D};INK4A$^{Lox/Lox}$;GPC1$^{+/+}$ or GPC1$^{-/-}$ transgenic mice that were 60 to 65 days old. Cells were then grown in DMEM supplemented with 20% FBS, penicillin/streptomycin (100U/ml) (Mediatech, Herndon, VA), heparin (100 μg/ml) (Sigma), endothelial cell growth factor (100 μg/ml) (Biomedical Technologies, Stoughton, MA), 1X non-essential amino acids (Gibco, Grand Island, NY), 2 mM L-glutamine (Gibco), 1X sodium pyruvate, gentamicin (58 μg/ml) (Gibco), and amphotericin B (25 ng/ml) (Mediatech), termed endothelial complete medium, and plated on fibronectin (1 μg/cm^2) coated plates (BD Biosciences).

Cell culture and in vitro assays

Anchorage-dependent growth was assessed by plating 3×10^3 primary cancer cells per well of a 96-well plate, serum starved overnight, incubated for 48 hours in serum free media (DMEM, 5 μg/ml apotransferrin, 5 ng/ml selenium, 0.01% BSA, and 100 U/ml penicillin/streptomycin) and then utilizing the 3-(4,5-methylthiazol-2-yl)-2,5-diphenyltetrazolium bromide (MTT) assay (Kleeff et al 1998). Doubling times were determined by plating 2×10^4 cells/well in 6-well plates and counting cells with a hemocytometer every 24 hours for five days.

BD Biocoat Matrigel Invasion Chambers (BD Biosciences, San Jose, CA) were utilized to assess cancer cell invasion. The chambers were incubated at room temperature for 30 min and rehydrated with 0.5 ml of serum free DMEM medium for 2 hours at 37°C. Cancer cells were seeded in each chamber at a cell density of 50×10^3 in 500 μl of serum free medium, and incubated for 22 hours at 37°C in a well containing 750 μl of serum free medium in the absence or presence of 50 ng/ml of FGF-2. After washing, fixing, and staining, cells were counted on an inverted microscope (10X objective).

Wounding assays were performed to assess the ability of immortalized MEFs to migrate in response to growth factors (Arnold et al 2004, Rowland-Goldsmith et al 2001). Briefly, 75×10^3 MEFs originally isolated from GPC1$^{+/+}$ or GPC1$^{-/-}$ mice were plated in each well of a 6-well plate and serum starved overnight. Confluent cells were washed with HBSS, a p200 pipet tip was used to make two scratches across each well, the cells were gently washed again, and incubated in serum free medium in the absence or presence of 75 ng/ml of FGF-2 or VEGF-A. Photos taken at 0 and 8 hours allowed for analysis of the migration distance (Suyama et al 2003).

Transwell migration assays were used to analyze the ability of primary endothelial cells to migrate in response to HBGFs. For these assays, transwell chambers (BD Biosciences) were coated by overnight incubation at 4°C with 100 μl of the purified matrix proteins: 1.5 μg/ml collagen (Cohesion, Palo Alto, CA), 0.5 μg/ml vitronectin (Sigma), 5 μg/ml fibronectin (BD Biosciences), and 0.5% gelatin. The primary endothelial cells were serum starved overnight.

After removal of the matrix protein solution, the chambers were saturated with 100 μl of 1% BSA in PBS and incubated for 1 hour at 37°C. The BSA was removed and 10×10^4 endothelial cells isolated from GPC1$^{+/+}$ or GPC1$^{-/-}$ mice were added to each chamber using serum free endothelial growth medium. The chambers were moved to a well containing 600 μl of serum free medium and incubated for 12 hours in the absence or presence of VEGF-A. The cells were then fixed with 4% paraformaldehyde, stained with 1% toluidine blue and 2% sodium borate, and counted on an inverted microscope with the 20X objective (Neupane and Korc 2008).

Quantitative Real Time PCR analysis

To assess the impact of GPC1 on the expression levels of VEGF-A and GPC2-6, total RNA was isolated from tumors arising in 60 day old GPC1$^{+/+}$ and 5 GPC1$^{-/-}$ mice, using the low temperature guanidine isothiocyanate method (Chang et al 1990, Han et al 1987). The concentration of RNA was determined spectrophometrically and RNA integrity was verified on a 1% agarose gel. cDNA was synthesized using oligo-dT primers as part of the SuperScript RT kit (Invitrogen) according to the manufacturer's protocol. Quantitative real time RT-PCR (Q-PCR) was performed using an ABI Prism 7300 sequence detection system (Applied Biosystems, Carlsbad, CA) utilizing the Applied Biosystems Taqman Assay with pre-validated murine probes and primer sets. All RNA samples were run in duplicate and each experiment was repeated in triplicate. A dilution series was carried out for each gene and the 18S ribosomal subunit was used as an internal control. Q-PCR data were expressed as a relative quantity based on the ratio of fluorescent change observed with the 18S ribosomal subunit.

Orthotopic mouse models

To compare the tumorogenicity of the four primary mouse cancer cell lines isolated from GPC1$^{+/+}$ and GPC1$^{-/-}$ mice pancreatic tumors, GPC1$^{+/+}$ (F1015 and F1048) and GPC1$^{-/-}$ (J444 and J446) cells (5×10^6), were injected subcutaneously into athymic nude mice and assessed for tumors daily. To determine the consequences of GPC1 loss on the metastatic potential of the cancer cells, two small tumor fragments from 65 day old Pdx1-Cre;LSL-Kras^{G12D};INK4A$^{Lox/Lox}$;GPC1$^{+/+}$ or GPC1$^{-/-}$ transgenic mice were sutured into the pancreata of 4-6 athymic GPC1$^{+/+}$ or 4-6 GPC1$^{-/-}$ mice, respectively. Each orthotopic experiment was carried out in triplicate.

Microarray Analysis

Total RNA from five GPC1$^{+/+}$ and five GPC1$^{-/-}$ tumors isolated from 65 day old transgenic mice was extracted using Trizol (Invitrogen). Gene expression analysis and bioinformatics was performed by Miltenyi Biotec (Bergisch Gladbach, Germany) using two-color Agilent whole mouse genome arrays where each knockout sample was hybridized to a control sample on the same array and assignment of the Cy5/Cy3 pairs was arbitrary.

Author Manuscript

Statistics

For statistical group comparisons of array data between the knockout and control samples, unpaired t-tests with equal variance were employed utilizing the normalized intensity data. All other data were analyzed by Student's t test, with $p<0.05$ defined as significant.

Supplementary Material

Refer to Web version on PubMed Central for supplementary material.

Acknowledgements

References

Aguirre AJ, Bardeesy N, Sinha M, Lopez L, Tuveson DA, Horner J, et al. Activated Kras and Ink4a/Arf deficiency cooperate to produce metastatic pancreatic ductal adenocarcinoma. Genes Dev. 2003; 17:3112–3126. [PubMed: 14681207]

Aikawa T, Whipple CA, Lopez ME, Gunn J, Young A, Lander AD, et al. Glypican-1 modulates the angiogenic and metastatic potential of human and mouse cancer cells. J Clin Invest. 2008; 118:89–99. [PubMed: 18064304]

Arnold NB, Ketterer K, Kleeff J, Friess H, Buchler MW, Korc M. Thioredoxin is downstream of Smad7 in a pathway that promotes growth and suppresses cisplatin-induced apoptosis in pancreatic cancer. Cancer Res. 2004; 64:3599–3606. [PubMed: 15150118]

Bardeesy N, Aguirre AJ, Chu GC, Cheng KH, Lopez LV, Hezel AF, et al. Both p16(Ink4a) and the p19(Arf)-p53 pathway constrain progression of pancreatic adenocarcinoma in the mouse. Proc Natl Acad Sci U S A. 2006; 103:5947–5952. [PubMed: 16585505]

Berman B, Ostrovsky O, Shlissel M, Lang T, Regan D, Vlodavsky I, et al. Similarities and differences between the effects of heparin and glypican-1 on the bioactivity of acidic fibroblast growth factor and the keratinocyte growth factor. J Biol Chem. 1999; 274:36132–36138. [PubMed: 10593896]

Blackhall FH, Merry CL, Davies EJ, Jayson GC. Heparan sulfate proteoglycans and cancer. Br J Cancer. 2001; 85:1094–1098. [PubMed: 11710818]

Cepko, CP.; Warren. Retrovirus infection of Cells in vitro and in vivo. Wiley Interscience; 1996. Current Protocols in Molecular Biology.; p. 9.14.11-19.14.16.

Chang SC, Brannon PM, Korc M. Effects of dietary manganese deficiency on rat pancreatic amylase mRNA levels. J Nutr. 1990; 120:1228–1234. [PubMed: 1698952]

Chen RL, Lander AD. Mechanisms underlying preferential assembly of heparan sulfate on glypican-1. J Biol Chem. 2001; 276:7507–7517. [PubMed: 11106655]

Cheng N, Brantley DM, Liu H, Lin Q, Enriquez M, Gale N, et al. Blockade of EphA receptor tyrosine kinase activation inhibits vascular endothelial cell growth factor-induced angiogenesis. Molecular cancer research : MCR. 2002; 1:2–11. [PubMed: 12496364]

Ding K, Lopez-Burks M, Sanchez-Duran JA, Korc M, Lander AD. Growth factor-induced shedding of syndecan-1 confers glypican-1 dependence on mitogenic responses of cancer cells. J Cell Biol. 2005; 171:729–738. [PubMed: 16286510]

Gengrinovitch S, Berman B, David G, Witte L, Neufeld G, Ron D. Glypican-1 is a VEGF165 binding proteoglycan that acts as an extracellular chaperone for VEGF165. The Journal of Biological Chemistry. 1999; 274:10816–10822. [PubMed: 10196157]

Gu G, Brown JR, Melton DA. Direct lineage tracing reveals the ontogeny of pancreatic cell fates during mouse embryogenesis. Mech Dev. 2003; 120:35–43. [PubMed: 12490294]

Habbe N, Shi G, Meguid RA, Fendrich V, Esni F, Chen H, et al. Spontaneous induction of murine pancreatic intraepithelial neoplasia (mPanIN) by acinar cell targeting of oncogenic Kras in adult mice. Proc Natl Acad Sci U S A. 2008; 105:18913–18918. [PubMed: 19028870]

Han JH, Stratowa C, Rutter WJ. Isolation of full-length putative rat lysophospholipase cDNA using improved methods for mRNA isolation and cDNA cloning. Biochemistry. 1987; 26:1617–1625. [PubMed: 3593682]

Hingorani SR, Petricoin EF, Maitra A, Rajapakse V, King C, Jacobetz MA, et al. Preinvasive and invasive ductal pancreatic cancer and its early detection in the mouse. Cancer Cell. 2003; 4:437–450. [PubMed: 14706336]

Hwang RF, Moore T, Arumugam T, Ramachandran V, Amos KD, Rivera A, et al. Cancer-associated stromal fibroblasts promote pancreatic tumor progression. Cancer Res. 2008; 68:918–926. [PubMed: 18245495]

Jackson EL, Willis N, Mercer K, Bronson RT, Crowley D, Montoya R, et al. Analysis of lung tumor initiation and progression using conditional expression of oncogenic K-ras. Genes Dev. 2001; 15:3243–3248. [PubMed: 11751630]

Jen YH, Musacchio M, Lander AD. Glypican-1 controls brain size through regulation of fibroblast growth factor signaling in early neurogenesis. Neural Dev. 2009; 4:33. [PubMed: 19732411]

Johnson L, Greenbaum D, Cichowski K, Mercer K, Murphy E, Schmitt E, et al. K-ras is an essential gene in the mouse with partial functional overlap with N-ras. Genes Dev. 1997; 11:2468–2481. [PubMed: 9334313]

Kim I, Saunders TL, Morrison SJ. Sox17 dependence distinguishes the transcriptional regulation of fetal from adult hematopoietic stem cells. Cell. 2007; 130:470–483. [PubMed: 17655922]

Kleeff J, Ishiwata T, Kumbasar A, Friess H, Buchler MW, Lander AD, et al. The cell-surface heparan sulfate proteoglycan glypican-1 regulates growth factor action in pancreatic carcinoma cells and is overexpressed in human pancreatic cancer. J Clin Invest. 1998; 102:1662–1673. [PubMed: 9802880]

Kleeff J, Wildi S, Kumbasar A, Friess H, Lander AD, Korc M. Stable transfection of a glypican-1 antisense construct decreases tumorigenicity in PANC-1 pancreatic carcinoma cells. Pancreas. 1999; 19:281–288. [PubMed: 10505759]

Kleeff J, Beckhove P, Esposito I, Herzig S, Huber PE, Lohr JM, et al. Pancreatic cancer microenvironment. Int J Cancer. 2007; 121:699–705. [PubMed: 17534898]

Korc M. Pathways for aberrant angiogenesis in pancreatic cancer. Mol Cancer. 2003; 2:8. [PubMed: 12556241]

Korc M. Pancreatic cancer-associated stroma production. The American Journal of Surgery. 2007; 194:S84–S86. [PubMed: 17903452]

Lander AD, Nie Q, Wan FY. Do morphogen gradients arise by diffusion? Dev Cell. 2002; 2:785–796. [PubMed: 12062090]

Le Mercier M, Fortin S, Mathieu V, Roland I, Spiegl-Kreinecker S, Haibe-Kains B, et al. Galectin 1 proangiogenic and promigratory effects in the Hs683 oligodendroglioma model are partly mediated through the control of BEX2 expression. Neoplasia. 2009; 11:485–496. [PubMed: 19412433]

Li A, Cheng XJ, Moro A, Singh RK, Hines OJ, Eibl G. CXCR2-Dependent Endothelial Progenitor Cell Mobilization in Pancreatic Cancer Growth. Transl Oncol. 2011; 4:20–28. [PubMed: 21286374]

Matsuda K, Maruyama H, Guo F, Kleeff J, Itakura J, Matsumoto Y, et al. Glypican-1 is overexpressed in human breast cancer and modulates the mitogenic effects of multiple heparin-binding growth factors in breast cancer cells. Cancer Res. 2001; 61:5562–5569. [PubMed: 11454708]

Neupane D, Korc M. 14-3-3sigma Modulates pancreatic cancer cell survival and invasiveness. Clin Cancer Res. 2008; 14:7614–7623. [PubMed: 19047086]

Olive KP, Jacobetz MA, Davidson CJ, Gopinathan A, McIntyre D, Honess D, et al. Inhibition of Hedgehog signaling enhances delivery of chemotherapy in a mouse model of pancreatic cancer. Science. 2009; 324:1457–1461. [PubMed: 19460966]

Preis M, Korc M. Kinase signaling pathways as targets for intervention in pancreatic cancer. Cancer Biol Ther. 2010; 9

Rowland-Goldsmith MA, Maruyama H, Kusama T, Ralli S, Korc M. Soluble type II transforming growth factor-beta (TGF-beta) receptor inhibits TGF-beta signaling in COLO-357 pancreatic cancer cells in vitro and attenuates tumor formation. Clin Cancer Res. 2001; 7:2931–2940. [PubMed: 11555612]

Rowland-Goldsmith MA, Maruyama H, Matsuda K, Idezawa T, Ralli M, Ralli S, et al. Soluble type II transforming growth factor-beta receptor attenuates expression of metastasis-associated genes and suppresses pancreatic cancer cell metastasis. Mol Cancer Ther. 2002; 1:161–167. [PubMed: 12467210]

Schneider G, Schmid RM. Genetic alterations in pancreatic carcinoma. Mol Cancer. 2003; 2:15. [PubMed: 12605716]

Seeley ES, Carriere C, Goetze T, Longnecker DS, Korc M. Pancreatic cancer and precursor pancreatic intraepithelial neoplasia lesions are devoid of primary cilia. Cancer Res. 2009; 69:422–430. [PubMed: 19147554]

Siegel R, Ward E, Brawley O, Jemal A. Cancer statistics, 2011: The impact of eliminating socioeconomic and racial disparities on premature cancer deaths. CA: a cancer journal for clinicians. 2011; 61:212–236. [PubMed: 21685461]

Suyama E, Kawasaki H, Nakajima M, Taira K. Identification of genes involved in cell invasion by using a library of randomized hybrid ribozymes. PNAS. 2003; 100:5616–5621. [PubMed: 12719525]

Terris B, Blaveri E, Crnogorac-Jurcevic T, Jones M, Missiaglia E, Ruszniewski P, et al. Characterization of gene expression profiles in intraductal papillary-mucinous tumors of the pancreas. Am J Pathol. 2002; 160:1745–1754. [PubMed: 12000726]

Tuveson DA, Hingorani SR. Ductal pancreatic cancer in humans and mice. Cold Spring Harb Symp Quant Biol. 2005; 70:65–72. [PubMed: 16869739]

Vilar E, Salazar R, Perez-Garcia J, Cortes J, Oberg K, Tabernero J. Chemotherapy and role of the proliferation marker Ki-67 in digestive neuroendocrine tumors. Endocr Relat Cancer. 2007; 14:221–232. [PubMed: 17639039]

Vlodavsky I, Korner G, Ishai-Michaeli R, Bashkin P, Bar-Shavit R, Fuks Z. Extracellular matrix-resident growth factors and enzymes: possible involvement in tumor metastasis and angiogenesis. Cancer Metastasis Rev. 1990; 9:203–226. [PubMed: 1705486]

Vonlaufen A, Phillips PA, Xu Z, Goldstein D, Pirola RC, Wilson JS, et al. Pancreatic stellate cells and pancreatic cancer cells: an unholy alliance. Cancer Res. 2008; 68:7707–7710. [PubMed: 18829522]

Xu J. Preparation, culture, and immortalization of mouse embryonic fibroblasts. Curr Protoc Mol Biol Chapter. 2005; 28 Unit 28 21.

Zetser A, Bashenko Y, Edovitsky E, Levy-Adam F, Vlodavsky I, Ilan N. Heparanase induces vascular endothelial growth factor expression: correlation with p38 phosphorylation levels and Src activation. Cancer Res. 2006; 66:1455–1463. [PubMed: 16452201]
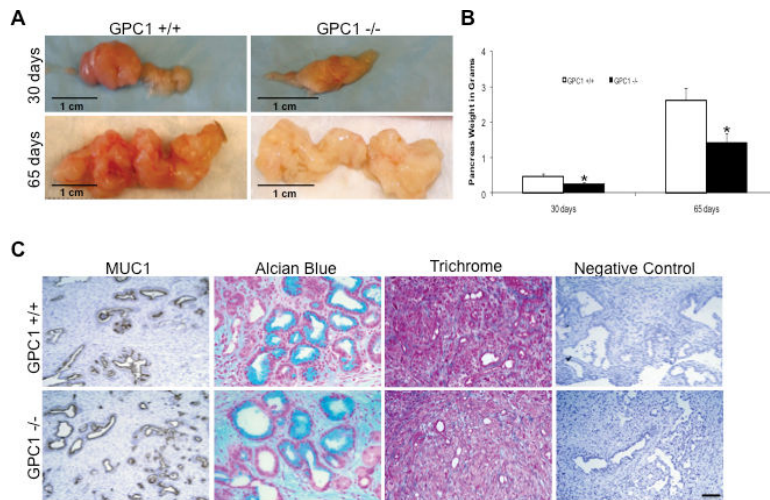
Figure 1.
Effects of glypican-1 loss on pancreas size and tumor morphology. **A**. Representative pancreata from 30 and 65 day old Pdx1-Cre;LSL-Kras^{G12D};INK4A/Arf$^{lox/lox}$;GPC1$^{+/+}$ or GPC1$^{-/-}$ transgenic mice. **B**. Pancreatic wet weight. Data are an average wet weight of 10 GPC1$^{+/+}$ and 10 GPC1$^{-/-}$ 30 day old mice, and 15 GPC1$^{+/+}$ and 20 GPC1$^{-/-}$ 65 day old transgenic mice. Data are the means ± SEM; *P < 0.05, when compared with corresponding GPC1$^{+/+}$ group. **C.** Pancreatic morphology. MUC1, Alcian blue, and Mason's-Trichrome staining were performed on paraffin sections (5 μm thick) prepared from indicated pancreatic tumors. Magnification 10X. Bar: 50 μM.

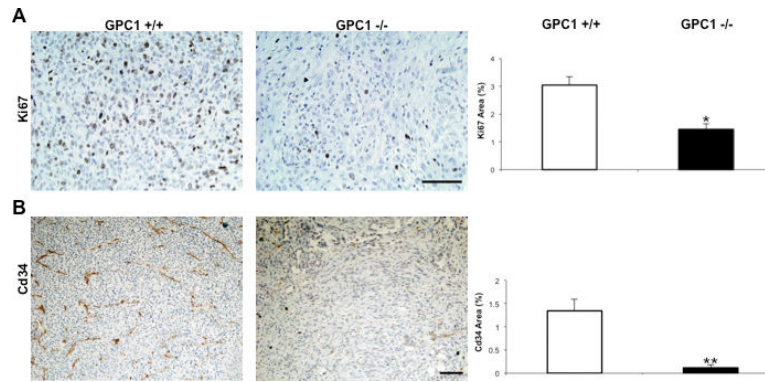**Figure 2.**
Effects of glypican-1 loss on Ki67 and CD34 immunoreactivity. **A**. Ki67 immunoreactivity. Staining was performed on paraffin sections (5 μm thick) prepared from indicated pancreatic tumors (6 mice in each group). **B.** CD34 immunoreactivity. CD34 immunostaining was analyzed in the indicated pancreatic tumors (7 mice in each group). Magnification 20X. **C**. Morphometric analysis. Quantitative morphometry was performed after scoring 12 areas on each slide prepared from the 26 tumors described in A and B. Magnification 10X. Data are the means ± SEM. *$P < 0.05$ and **$P < 0.002$, by comparison with respective values in the GPC1$^{+/+}$ tumors. Bar: 50 μM.
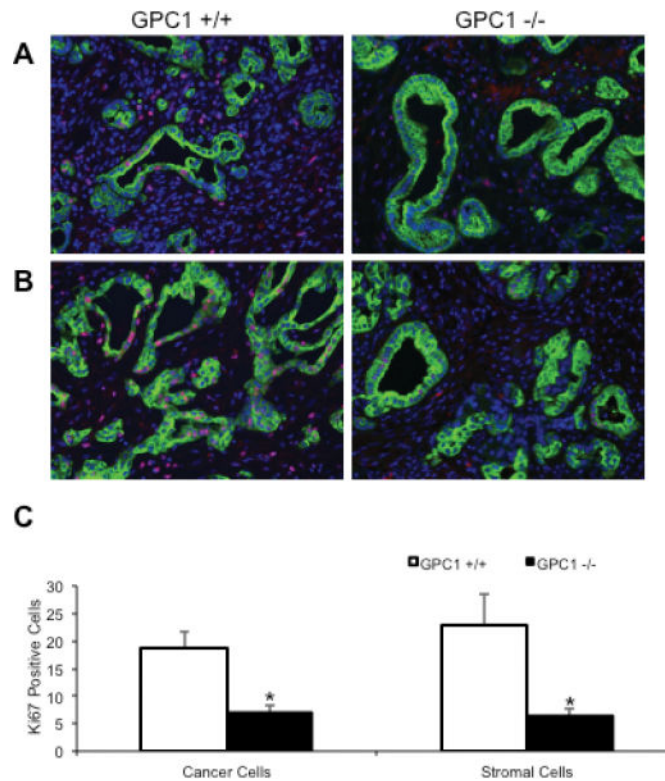
Figure 3.
Evaluation of cellular proliferation in cancer cells and adjoining stroma. **A**. Ki67 immunofluorescence. Immunofluorescent staining was performed on paraffin sections (5 μm thick) prepared from pancreatic tumors isolated from two tumors/group of 65 day old Pdx1-Cre;LSL-Kras^{G12D};INK4A/Arf$^{lox/lox}$;GPC1$^{+/+}$ or GPC1$^{-/-}$ mice. Ki67-positive cells (stained red) are seen in the cancer cells (arrow) in which the cells are also CK19-positive (stained green), and in the adjacent stromal cells (asterisks). Nuclei are stained with DAPI in blue. Magnification 20X. Bar: 50 μM.

B. Quantitative morphometry. Ki67 positive cancer cells and stromal fibroblasts were scored in 5 areas from each slide and expressed as a percent of the total number of cancer cells and stromal fibroblasts, respectively. Data are means ± SEM from 9 GPC1$^{+/+}$ and 9 GPC1$^{-/-}$ transgenic mice. *$P < 0.05$ when compared to the corresponding GPC1$^{+/+}$ group.
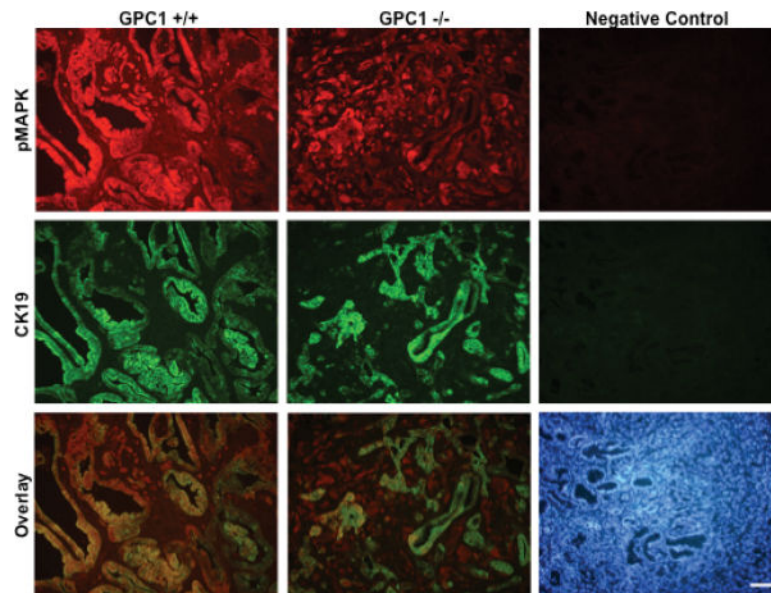
Figure 4.
Effects of glypican-1 on pMAPK immunofluorescence. pMAPK immunostaining was performed on paraffin sections (5 μm thick) prepared from pancreatic tumors isolated from 65 day old Pdx1-Cre;LSL-Kras^{G12D};INK4A/Arf$^{lox/lox}$ mice that were either GPC1$^{+/+}$ or GPC1$^{-/-}$. The slides were also stained for CK19 to identify the epithelial cells. Negative controls were stained in the absence of the respective primary antibody. Magnification 20X. Bar: 50 μM.
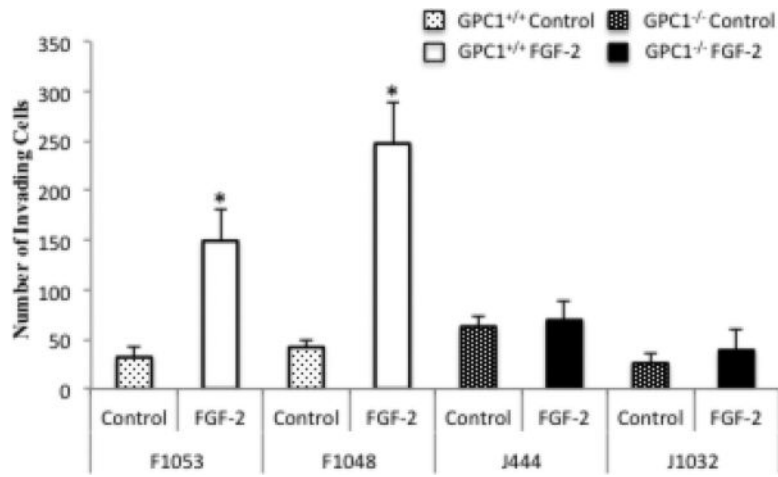
Figure 5.
Effects of GPC1 on primary cancer cell invasion. F1015 and F1048 cells, derived from
GPC1^{+/+} tumors, and J444 and J1032 cells, derived from GPC1^{-/-} tumors, were incubated
for 22 hours in serum free medium, in the absence or presence of 75 ng/ml of FGF-2. Data
are expressed as the total number of cells that invaded in response to 0.1% BSA (control) or
FGF-2 and are the means ± SEM from 3 separate experiments. *$P < 0.05$, when compared
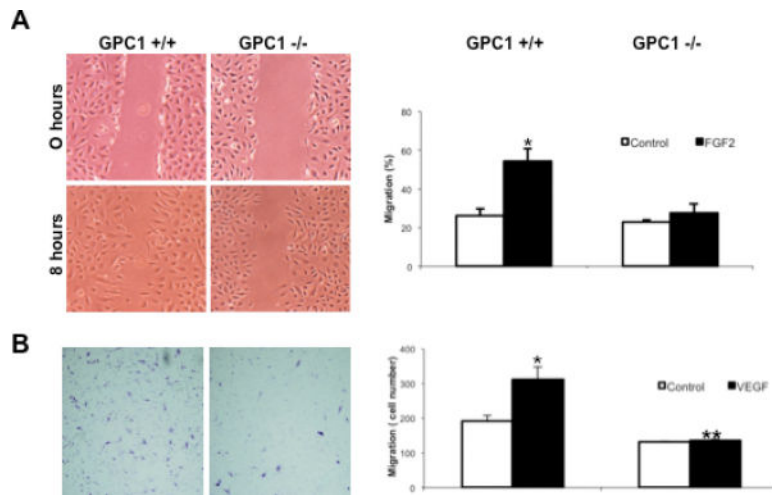with the corresponding control.

Figure 6.
Effects of GPC1 on cell migrations. **A**. Migration of immortalized MEFs. Cells that were originally derived from GPC1$^{+/+}$ or GPC1$^{-/-}$ mice were serum starved overnight and then incubated for 8 hours with 75 ng/ml FGF-2. Representative photos are shown at 0 hours and 8 hours following FGF-2 addition. Bar graphs on the right are the means +/- SEM of duplicate determinations from 3 separate experiments. *$p < 0.05$ by comparison with respective control in the absence of FGF-2. **B.** Migration of primary hepatic endothelial cells. Endothelial cells were incubated overnight in the absence or presence of 75 ng/ml of VEGF-A. Representative photos are of endothelial cells derived from GPC1$^{+/+}$ or GPC1$^{-/-}$ mice. Bar graphs on the right are the means +/- SEM of duplicate determinations from 3 separate experiments. *$p < 0.05$ by comparison with respective control in the absence of FGF-2.

Table 1

Effects of the loss of GPC1 on tumor metastasis

Mouse	WT	KO
Mice with mesenteric metastases (>100 per mouse)	9/15	2/14
Mice with renal metastases (3-5 per mouse)	3/15	0/14

Tumor fragments isolated from pancreatic cancers arising in GPC1$^{+/+}$ or GPC1$^{-/-}$ mice were inserted into the pancreas of GPC1$^{+/+}$ or GPC1$^{-/-}$ athymic mice, respectively. Metastasis was assessed three weeks later.

Table 2

Effects of GPC1 loss on expression of pro-angiogenic genes

Gene	Micro-array Fold Change	Q-PCR Fold Change
EFNA1	-5.4	-3.6
CX3CL1	-6.9	-3.2
PTK2B	-4.7	-3.1
GNA13	-5.4	-2.3
VEGFA	-4.3	-3.5
SOX17	-6.8	-7.8
ITGB3	-4.9	-2.4

RNA isolated from pancreatic tumors derived from 5 GPC^{+/+} and 5 GPC1^{-/-} mice was analyzed using an Agilent 4X44K Whole Mouse Genome Oligo Microarray. Pro-angiogenesis genes down-regulated in the GPC1^{-/-} mice are shown above (full names are listed in supplemental figure 3). Microarray data were validated by Q-PCR, which was performed in triplicate. All data were significantly different from corresponding values in GPC1^{+/+} tumors ($p < 0.05$).